Likely Impact of the Approaching Solar Maximum on GNSS Surveys: Be Alert but Not Alarmed

Volker Janssen
Survey Infrastructure and Geodesy, Land and Property Information
NSW Department of Finance & Services
Volker.Janssen@lpi.nsw.gov.au

ABSTRACT

Global Navigation Satellite System (GNSS) signals travel about 20,000 km from the satellite to a receiver on the surface of the Earth. At the end of this journey, which only takes about 60-70 milliseconds, the GNSS signal must travel through the Earth's atmosphere. Particularly the ionosphere, located at a height of between about 50 and 1,000 km above the surface, has a significant effect on the propagation of GNSS signals due to its high spatial and temporal variability. Most of the ionosphere is electrically neutral, but when solar radiation strikes it becomes an electrical conductor and supports the flow of electric currents. The effect of the ionosphere on GNSS signal propagation is a function of the Total Electron Content (TEC) along the signal path and the frequency of the signal. The TEC varies with time, season and geographic location. When travelling through the ionosphere, the speed of the GNSS signal deviates from the speed of light, causing measured pseudoranges to be 'too long' compared to the geometric distance between satellite and receiver, while carrier-phase observations are 'too short'. The condition of the ionosphere is strongly related to the solar cycle, which shows a maximum approximately every 11 years. This paper discusses the likely effects of the maximum of the current solar cycle (cycle 24), predicted to occur in early 2013, on GNSS users. Although it is anticipated to be a smaller solar maximum than the previous peak encountered in 2000-2001, GNSS users can at times expect reduced positioning, navigation and timing performance. Particularly during enhanced ionospheric or geomagnetic storm activity caused by sudden eruptions of the Sun, increased ionospheric variability can be expected. This will also cause increased scintillation effects (i.e. rapid changes in the phase and amplitude of the transmitted signals), which adversely affects ambiguity resolution and may cause GNSS receivers to lose lock in some instances.

KEYWORDS: *Solar cycle, ionospheric delay, TEC, scintillations, GNSS.*

1 INTRODUCTION

Global Navigation Satellite System (GNSS) signals travel about 20,000 km from the satellite to a receiver on the surface of the Earth. This journey only takes about 60-70 milliseconds (0.06-0.07 seconds) and requires the GNSS signal to travel through the Earth's atmosphere. The ionosphere is part of the Earth's upper atmosphere and stretches from a height of about 50 km to more than 1,000 km above the surface. Its high spatial and temporal variability has a significant effect on GNSS signals. Moreover, the condition of the ionosphere is strongly related to the solar cycle, which shows a maximum approximately every 11 years.

The effects of the ionosphere can be breathtakingly beautiful, i.e. the aurora australis/borealis (the southern/northern lights) are dancing curtains of light that occur when charged particles

enter the Earth's atmosphere at high latitudes. On the other hand, the effects can also be devastating, i.e. solar storms can cause widespread power blackouts, disrupt navigation systems and radio communication, and destroy the payloads on commercial satellites.

The ionosphere is the largest individual systematic error in the GNSS error budget, accounting for as much as 80% or more (Kunches and Klobuchar, 2001). The ionospheric range error on the GPS L1 frequency in the zenith direction can reach 30 metres or more, and near the horizon this effect is amplified by a factor of about three (Teunissen and Kleusberg, 1998). The ionosphere may also cause intermittent signal fading, in severe cases causing losses of availability. Travelling ionospheric disturbances can move at speeds of up to 1,000 m/s, causing sudden changes in electron density. In addition, ionospheric scintillations, which manifest themselves as rapid phase and amplitude variations of the received signal, can cause GNSS receivers to lose lock, thereby interrupting the reception of one or more satellites (ESA, 2005).

At present we are approaching another solar maximum, which is currently predicted to occur in early 2013. This has led to increased interest regarding the possible effects on GNSS users (e.g. Kintner et al., 2009; Jensen and Mitchell, 2011). This paper briefly explains how the occurrence of sunspots and the solar cycle influence the behaviour of the ionosphere. Related phenomena such as scintillations, travelling ionospheric disturbances and ionospheric storms are described, and recent advances in modelling the ionosphere are outlined. Finally, the likely effects of the maximum of the current solar cycle (cycle 24) on GNSS users are discussed, with an emphasis on Australia.

2 SUNSPOTS AND THE SOLAR CYCLE

Sunspots are the physical expression of complex processes within the Sun and are seen as dark areas on the solar disk that wax (become stronger) and wane (become weaker) (Figure 1). Sunspots are darker than their surrounding area because they are cooler than the average temperature of the solar surface and can therefore easily be observed. The appearance and disappearance of sunspots is due to underlying changes in the magnetic fields that exist throughout the Sun. For an extensive review on sunspots, the reader is referred to Solanki (2003).

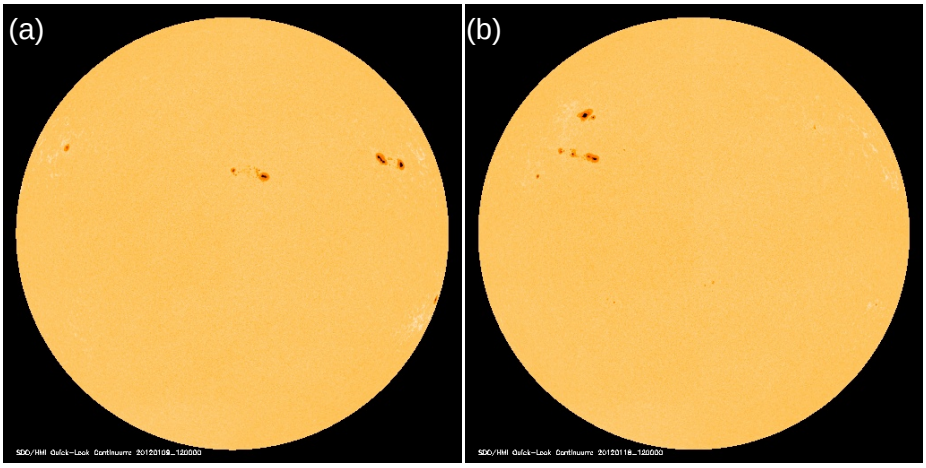

Figure 1: Sunspots on (a) 9 January 2012 at 12:00 UT and (b) 18 January 2012 at 12:00 UT (NASA, 2012a).

The pattern of sunspots on the Sun varies on timescales from a few hours to many years. In order to quantify the abundance of spots, an index called the *sunspot number* was introduced about 400 years ago and has been used to consistently and continuously monitor sunspots for the last 260 years. The sunspot number is calculated from the number of individual sunspots and sunspot groups visible on the Sun, under consideration of differences between observers and observatories.

In this context it is necessary to clarify a few terms associated with solar activity. As explained by Knight (2000), sudden increases in the intensity of solar radiation associated with sunspot activity are known as *solar flares*. The *solar wind* is composed of particles charged with high energy that are emitted from the Sun. *Coronal holes* are low density regions of the solar corona (region around the Sun, extending more than one million kilometres from its surface) and the primary source of the solar wind.

The solar cycle has an average length of 11 years. However, cycles vary considerably in length from as short as 9 years up to almost 14 years. Due to its large day-to-day variability, the sunspot number is usually averaged over a month. If smoothed over a 13-month period, it effectively charts the progress of the solar cycle. The daily and monthly averages exhibit considerable variation with respect to the smoothed curve due to bursts of rapid solar region growth often associated with events like solar flares. Figure 2 shows the smoothed sunspot numbers for the entire 260-year historical record, i.e. solar cycles 1-23.

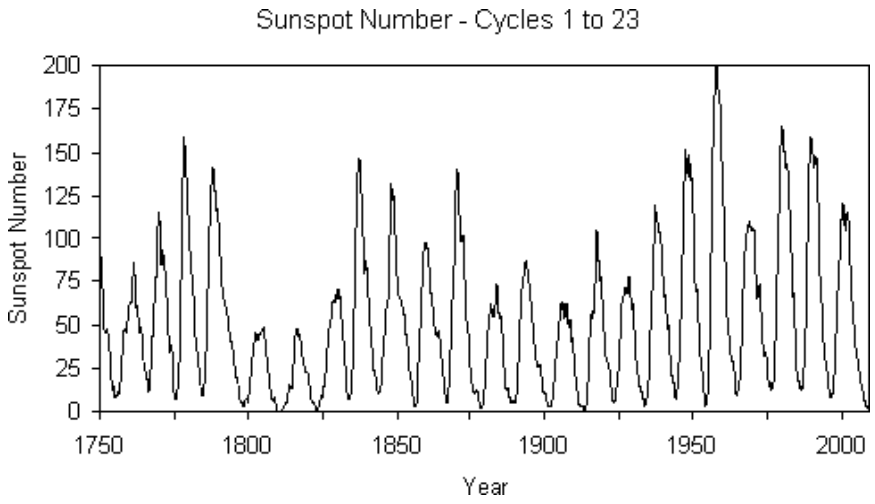

Figure 2: General variation of the solar cycles (1-23), illustrated by the smoothed sunspot number (IPS, 2012a).

At present, we are more than three years into the current solar cycle (cycle 24). Increased activity in the last few months has raised the predicted maximum and moved it to occur earlier than first expected. The solar maximum is now predicted to occur in early 2013, although this may still be revised by several months. It should be noted that ionospheric activity tends to remain high for several years around the solar maximum. However, the currently predicted size (smoothed sunspot number maximum of about 59) still makes this the smallest solar cycle in about 100 years. Figure 3 illustrates the monthly sunspot numbers for the previous solar cycle 23 (with its maximum in 2000-2001) and the current solar cycle 24, including a prediction for the remainder of the cycle.

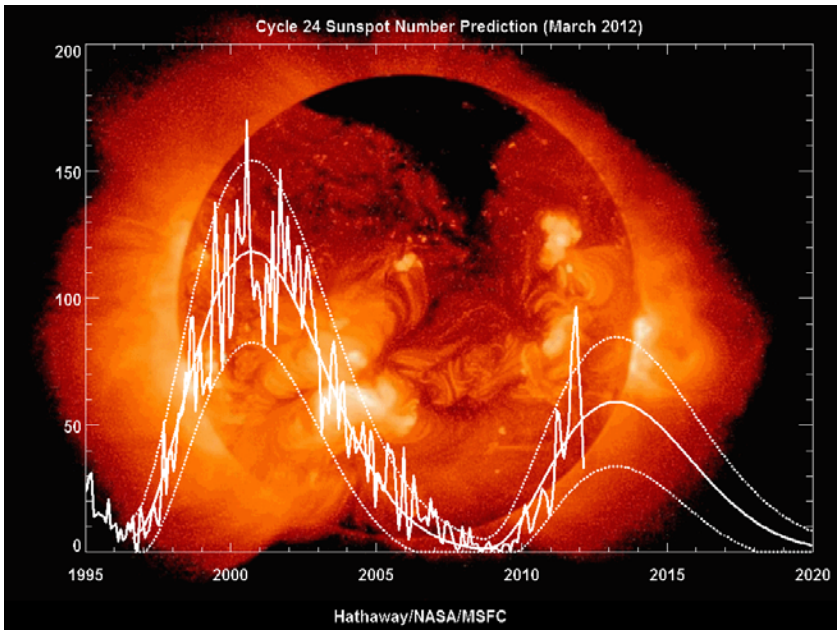

Figure 3: Monthly sunspot numbers for solar cycles 23 and 24, including prediction (NASA, 2012b).

3 THE IONOSPHERE

The ionosphere is a band of the atmosphere located about 50-1,000 km above the Earth's surface, thinning into the plasmasphere (or protonosphere) and eventually into the interplanetary plasma at greater heights. Most of the ionosphere is electrically neutral, but ionisation (i.e. adding or subtracting electrons from atoms by strong electric fields in a gas) results when solar radiation strikes the ionosphere. The upper atmosphere then becomes an electrical conductor, which supports the flow of electric currents, and hence affects the propagation of radio waves.

Free, negatively charged, electrons are produced when solar radiation collides with uncharged atoms and molecules, leaving behind positively charged atoms (i.e. ions). This process only occurs in the daylight hemisphere of the ionosphere because it relies on solar radiation. On the other hand, a loss of free electrons in the ionosphere occurs when a free electron combines with an ion to form a neutral particle. Loss of electrons occurs continually, both day and night (Figure 4).

The ionosphere is traditionally divided into several regions (D, E and F) and layers, based on the level of ionisation within a region. Figure 5 illustrates these ionospheric layers and the principle ions that compose each region; the electron density is also included (in units of electrons/cm^3). The F2 layer is particularly important for GNSS users because here the electron concentrations reach their highest values.

The free electrons present in the ionosphere affect the propagation of radio waves. At frequencies of up to about 30 MHz the ionosphere acts almost like a mirror, bending the path travelled by a radio wave back towards the Earth, thereby allowing long-distance radio communication (e.g. 'over the horizon' via 'skips and hops'). At higher frequencies, such as those used by GNSS, radio waves pass right through the ionosphere. However, the speed of the GNSS signal deviates from the speed of light when travelling through the ionosphere. This causes measured pseudoranges to be 'too long' compared to the geometric distance

between satellite and receiver, while carrier-phase observations are 'too short'. The terms *group delay* and *phase advance* are also used in this context (Teunissen and Kleusberg, 1998).

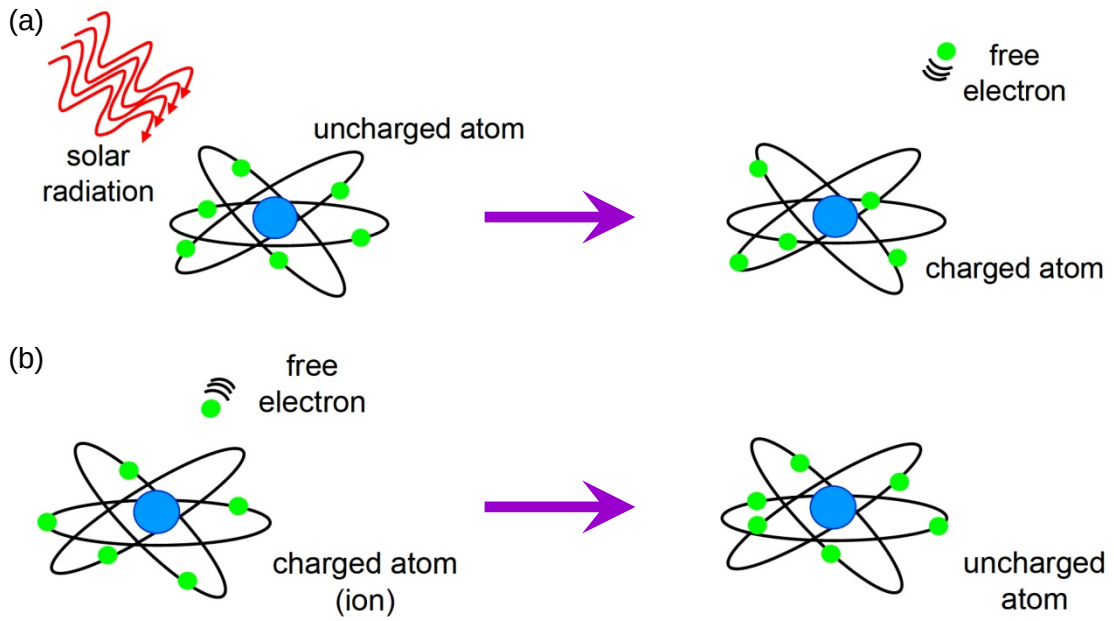

Figure 4: (a) Production and (b) loss of free electrons in the ionosphere (IPS, 2012b).

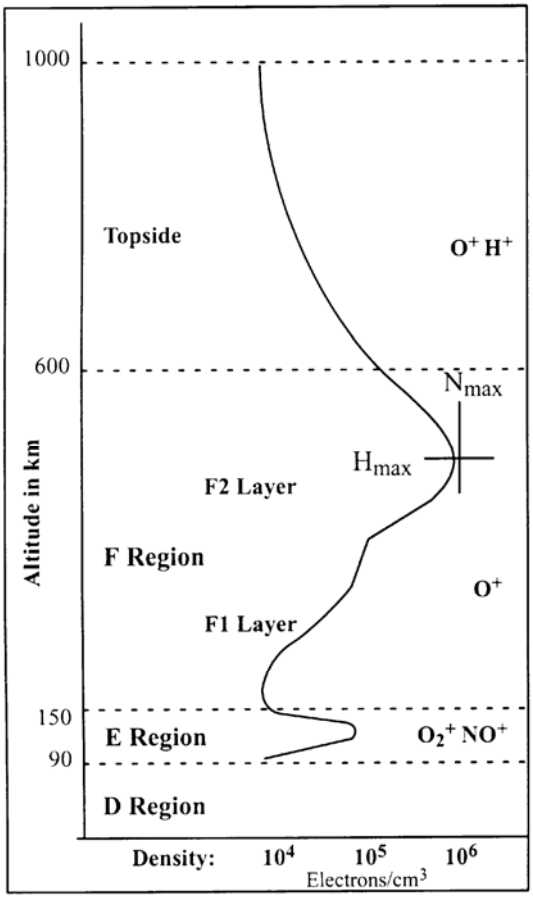

Figure 5: Regions and layers of the ionosphere, their predominant ion populations and electron density (Anderson and Fuller-Rowell, 1999).

The ionosphere is a dispersive medium for microwaves, i.e. the refractivity depends on the frequency of the propagating signal (e.g. Langley, 2000). Hence, measurements on multiple frequencies can be used to account for the ionospheric effect on GNSS observations, e.g. by forming the so-called ionosphere-free linear combination of the L1 and L2 signals. For short baselines the ionospheric effect is considered to be the same for both receivers, and therefore assumed to be eliminated by differencing the measurements taken at both ends. However, this assumption is not always true, particularly in periods of high solar activity. Experiments in Hong Kong have clearly shown that the ionospheric gradient in the region and the ionospheric delay effects could not be removed by double-differenced observables, even over baselines less than 10 km (Chen et al., 2001).

3.1 TEC

The effect of the ionosphere on GNSS signal propagation is a function of the Total Electron Content (TEC) along the signal path and the frequency of the signal. TEC is a measure of the integrated (i.e. summated or total) free electron density in a $1m^2$ column along the signal path between satellite and receiver, expressed in TEC units with 1 TECU = 1016 electrons/m^2. The TEC is highly variable with time, season and geographic location, with the main influences on signal propagation being solar activity and the Earth's magnetic field. Other factors influencing the ionospheric refraction are geographic location, the period in the solar cycle and the time of day. The largest TEC values are generally observed in the early afternoon local time, when the effect of solar radiation has reached a maximum. Consequently, the lowest activity is experienced late at night, just before sunrise (Jensen and Mitchell, 2011).

3.2 Scintillations

The ionosphere is most active in a band extending up to approximately 20° on either side of the geomagnetic equator (Figure 6). This is also one of the two regions where small-scale ionospheric disturbances (scintillations) mainly occur, the other being the high-latitude (auroral) regions close to the poles.

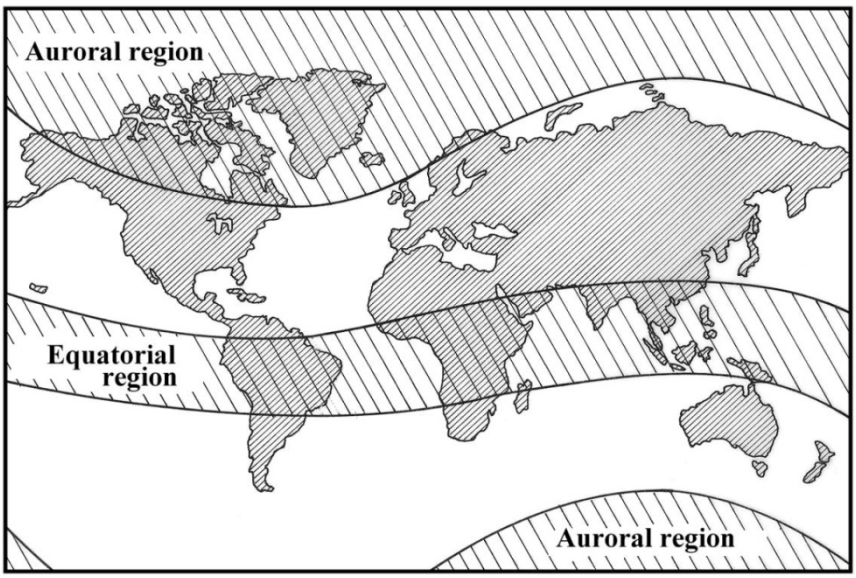

Figure 6: Regions of the world with high ionospheric activity (Seeber, 2003).

Scintillations are rapid, short-term variations in the amplitude and phase of radio signals travelling through the ionosphere, thereby causing rapid changes in signal power. Auroral and

polar scintillations are mainly the result of geomagnetic storms that are associated with solar flares and coronal holes. Equatorial scintillations, on the other hand, are caused by irregularities in the F-layer of the ionosphere following the passage of the *evening terminator*, the boundary that divides day from night (Knight, 2000). Equatorial scintillations generally occur from about one hour after sunset until midnight and should have disappeared by 03:00 local time (Klobuchar, 1996).

Figure 7 illustrates the maximum L-band signal fading depths (i.e. fading signal strength) due to ionospheric scintillation that can be expected during the peak of the solar cycle (left) and under solar minimum conditions (right). It can clearly be seen that scintillation effects are much more severe during solar maximum conditions. It should also be noted that the main anomaly region located at ±15° of the geomagnetic equator experiences the deepest signal fades of up to 20 dB below the mean signal level. Less intense fading is experienced at the geomagnetic equator and in regions surrounding the main anomaly region. The primary diurnal maximum of this *equatorial anomaly* is also known as the *fountain effect* because it is characterised by high electron concentration observed on either side of the geomagnetic equator.

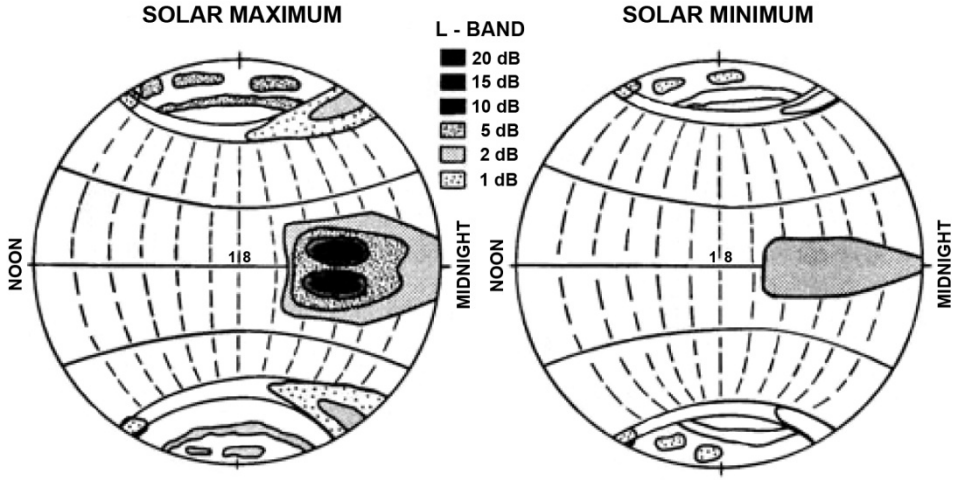

Figure 7: Ionospheric scintillations during high and low solar activity (Goodman and Aarons, 1990).

The occurrence of scintillations also varies with the seasons. Between April and August they are less severe in the American, African and Indian longitude regions, but are at a maximum in the Pacific region, while the situation is reversed from September to March (e.g. Seeber, 2003). It has also been shown that scintillation effects tend to peak in the equinox seasons, i.e. around 20-21 March and 22-23 September each year (Doherty et al., 2000).

3.3 Travelling Ionospheric Disturbances

Travelling ionospheric disturbances (TIDs) are wave-like density fluctuations that propagate through the ionosphere at various horizontal velocities and wavelengths of several hundred kilometres (Hocke and Schlegel, 1996). Generally, the distinction is made between large-scale TIDs (LSTIDs) and medium-scale TIDs (MSTIDs). LSTIDs are related to geomagnetic disturbances (e.g. caused by the aurora effect or ionospheric storms) and can travel large distances. They last for more than 1 hour and move faster than sound (i.e. in excess of 300 m/s or 1,080 km/h). On the other hand, MSTIDs are more related to lower atmospheric weather disturbances (e.g. severe weather fronts or volcanic eruptions). They last for shorter time periods (from 10 minutes to 1 hour) and move at slower speeds of about 50-300 m/s (e.g.

Hernández-Pajares et al., 2006; Wang et al., 2007). MSTIDs frequently occur in mid-latitudes, mainly during daytime in the winter months, during periods of high solar activity (e.g. Wanninger, 2004; Kotake et al., 2007).

3.4 Ionospheric Storms

Ionospheric storms result from large energy input to the upper atmosphere associated with geomagnetic storms. The latter are large variations in the strength and direction of the Earth's magnetic field caused by eruptions on the Sun that eject a mixture of electrons, protons and ions into the solar wind (Knight, 2000). Since the geomagnetic field and the ionosphere are linked in complex ways, a disturbance in the geomagnetic field often causes a disturbance in the ionosphere through fluctuations in electron density. This process can cause strong scintillation effects and large rapid changes in the ionospheric delay for GNSS signals, within time periods of about one minute. These ionospheric storms may last a number of days, and higher latitudes are generally affected more than low latitudes (IPS, 2012b).

4 MODELLING THE IONOSPHERE

Many different methods for estimating and modelling the ionospheric signal delay have been developed (e.g. Allain and Mitchell, 2009; Burrell et al., 2009). The ionosphere is usually approximated by a very thin shell at a certain altitude (generally between 300 and 400 km) above the Earth's surface. The slant TEC (STEC, along the line-of-sight to the satellite) is often converted to an equivalent vertical TEC (VTEC), allowing convenient comparison between different datasets and spatial mapping of the ionosphere (Figure 8). The point where the line of sight between a GNSS receiver and a satellite passes through this shell is known as the ionospheric pierce point (IPP).

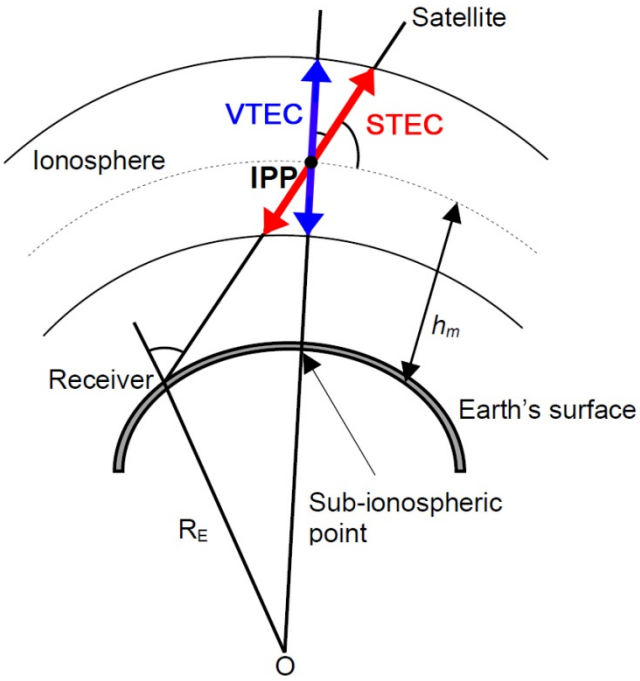

Figure 8: Geometry of a single-layer ionospheric shell model at altitude h_m, adapted from Ya'acob et al. (2008).

This single-layer approach is feasible because the majority of free electrons in the ionosphere are distributed at these altitudes. However, such a 2-dimensional model is not ideal because it

is unable to provide a vertical profile of the ionosphere. Alternatively, tomographic imaging (a medical imaging technique to create images of a parameter from integrated measurements) can be used (Bust and Mitchell, 2008). A tomographic model can describe the ionosphere in a 3-dimensional frame, allowing more precise exploration of the ionospheric characteristics and subsequently better modelling accuracy (Gao and Liu, 2002).

In practice, these two approaches for ionospheric modelling can be applied in two ways. The first option is to use a model *predicting* the ionospheric delay, e.g. the Klobuchar (1987) model or the International Reference Ionosphere (IRI) model (Bilitza, 2006). The coefficients for the Klobuchar (1987) model are determined by the GPS control segment and broadcast to users as part of the GPS navigation message. The second option is to implement *real-time mapping* and to transmit this information to the GNSS user in the field, e.g. via a geostationary satellite broadcasting on GNSS frequencies or the internet. Real-time mapping generally provides greater accuracy over prediction models. However, it does require a sufficiently dense GNSS Continuously Operating Reference Station (CORS) network infrastructure over the area of interest.

Considerable progress has been made in regards to improve modelling by accounting for second-order (i.e. non-linear) ionospheric terms (e.g. Hernández-Pajares et al., 2007; Hoque and Jakowski, 2008), which is particularly useful in periods of high solar activity. In addition, the ability to estimate ionospheric delay parameters quickly and precisely is expected to improve significantly when GPS observations can be combined with measurements using other GNSS such as GLONASS, Beidou and Galileo (Richert and El-Sheimy, 2005).

The introduction of new GNSS frequencies is expected to provide better ionospheric modelling over longer baselines. For example, the new dual-frequency GPS L1/L5 signal combination has a larger frequency separation than the original GPS L1/L2 combination, thereby promoting better correction of ionospheric effects (Roberts, 2011). Similarly, triple-frequency observations based on a single GNSS will allow instantaneous ambiguity resolution over longer distances. Traditional dual-frequency combinations must either compute a baseline solution whilst ignoring the ionosphere or vice versa. Triple-frequency combinations, on the other hand, will allow multiple combinations to compute the baseline and account for the ionosphere, thereby providing instantaneous positioning over longer baselines (Rizos, 2008).

The growing number of operational GNSS constellations also has the potential to generate new alternatives for GNSS positioning. For example, single-frequency code-plus-carrier positioning could become an interesting application of a future Galileo E5 receiver, due to the exclusive properties of this broadband signal. Simulated results featuring high ionospheric variations have indicated a positioning performance which is at least three times better than that of a GPS L1 receiver (Schüler et al., 2011).

4.1 Global Ionosphere Maps

The Center for Orbit Determination in Europe (CODE), located at the University of Bern in Switzerland, generates daily global ionosphere maps (GIMs) based on data collected at global International GNSS Service (IGS) sites (Schaer et al., 1998). An example of such a GIM is shown in Figure 9, dark blue indicating low TEC and red indicating high TEC. The dotted line corresponds to the geomagnetic equator. The equatorial anomaly (see section 3.2) is clearly visible north of Australia.

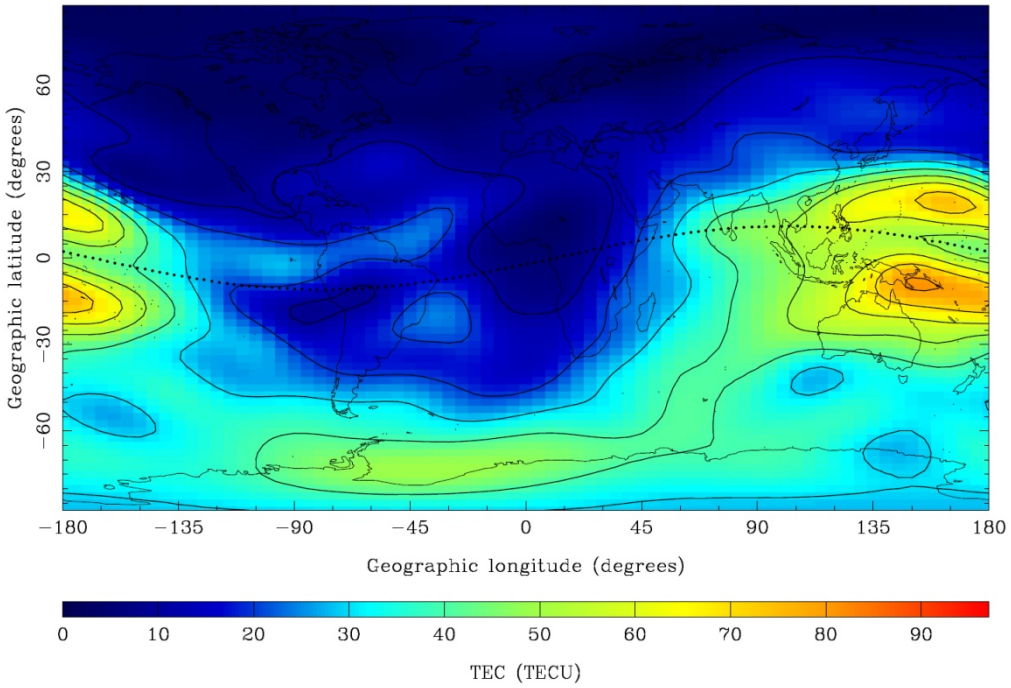

Figure 9: Global Ionosphere Map (GIM) for day 361, 2011 at 04:00 UT (AIUB, 2012).

While freely available on the internet, these global maps are not very effective in modelling the ionospheric conditions in local or regional GNSS networks for short observation periods because they cannot reproduce local, short-lasting processes in the ionosphere. Moreover, even though there are a large number of IGS sites, they are unevenly distributed, with most of the GNSS stations being situated in the mid-latitude region of the northern hemisphere. The smaller number of GNSS receivers in the equatorial region and the southern hemisphere, and consequently the reduced number of available TEC measurements, results in the ionospheric modelling to be less accurate for these regions. However, GIMs are invaluable for tracking the behaviour of the global ionosphere over time.

4.2 Regional Ionosphere Maps

The temporal and spatial TEC variations over a local or regional area are very complex, making it a challenging task to precisely represent the varying behaviour of the ionosphere (Wu et al., 2006). Nevertheless, many methods have been developed and evaluated to model the regional ionosphere based on GNSS observations (e.g. Gao and Liu, 2002; Janssen and Rizos, 2003; Wielgosz et al., 2003; Liu et al., 2011).

The Ionospheric Prediction Service (IPS), located in Sydney, Australia, produces near real-time regional ionospheric TEC maps for the Australasian region. These maps are determined by combining GPS data from a range of CORS with the IRI-2007 ionospheric model driven by real-time observations from IPS ionosondes. A brief description of ionosode operation can be found in IPS (2012b). An example of an IPS TEC map is shown in Figure 10, dark blue again representing low TEC while red indicates high TEC. It can clearly be seen that Australia is affected by the equatorial anomaly (04:30 UT is equivalent to 15:30 AEDST).

Time sequences of such TEC maps based on GNSS CORS network observations can also be used to investigate the spatial structure and temporal evolution of TIDs, geomagnetic storms and other ionospheric phenomena (e.g. Tsugawa et al., 2007; Wang et al., 2007).

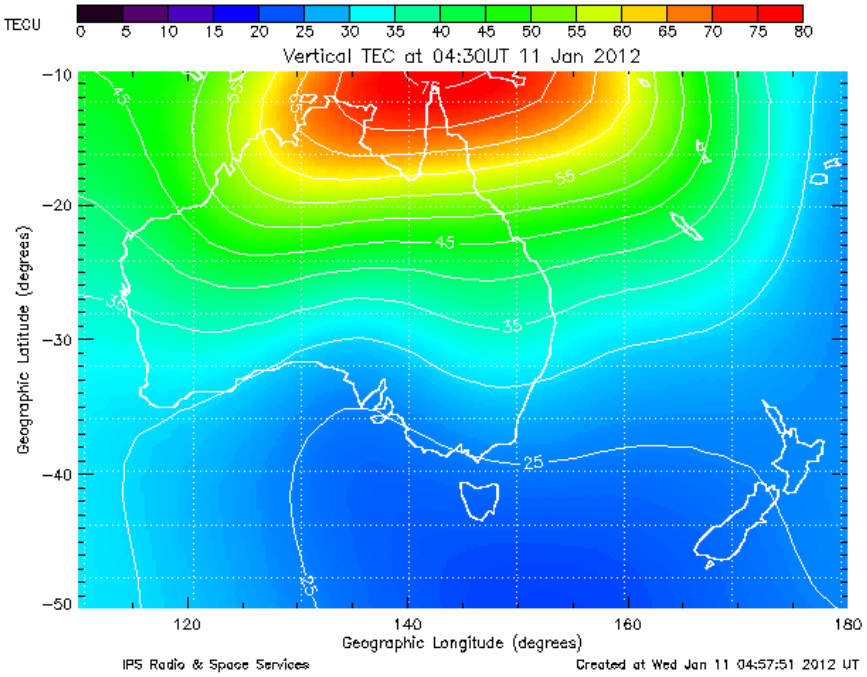

Figure 10: Regional Ionosphere Map for Australia for day 011, 2012 at 04:30 UT (IPS, 2012c).

5 LIKELY EFFECTS OF THE SOLAR MAXIMUM ON GNSS SURVEYS

Although the approaching maximum of solar cycle 24 is anticipated to be much smaller than the previous peak (see Figure 3), GNSS users can at times expect reduced positioning, navigation and timing performance. Particularly during enhanced ionospheric storm activity, increased TEC variability can be expected. The increased occurrence of scintillations, TIDs and ionospheric storms can lead to more cycle slips and (partial or complete) loss-of-lock for GNSS receivers as they track the signal, thereby limiting the availability of carrier-phase measurements and negatively affecting ambiguity resolution (e.g. longer time to fix ambiguities and lower success rate). In addition, the noise level of solutions is expected to rise for both pseudorange and carrier-phase observations during the solar maximum period. This may be noticeable, for example, through poorer standard deviations, reference variances, Root Mean Square (RMS) values, Quality Control (QC) or Coordinate Quality (CQ) values, and ratio tests.

5.1 Indications from International Studies

Scintillation effects mainly occur in the equatorial region (including Northern Australia) and at high latitudes, and are significantly more severe under solar maximum conditions (e.g. Datta-Barua et al., 2003; Seo et al., 2007). Analysing three years of GPS observations in Hong Kong during the previous solar maximum, Chen et al. (2008) showed that the number of loss-of-lock occurrences increased dramatically during strong disturbance periods (from less than 50 to 500 per day), with most losses occurring on the (weaker) L2 frequency. In addition, both the pseudorange and carrier-phase measurement noise level increased significantly. For the ionosphere-free combination, the carrier-phase measurement noise level increased by more than a third compared to ‘normal’ conditions. It was also shown that different types of GPS receivers behave differently during the disturbances, which is related to the receiver hardware and firmware employed.

Travelling ionospheric disturbances frequently occur in mid-latitudes and are more severe during periods of high solar activity. Australia is located mainly in the mid-latitude region. Consequently, MSTIDs have the biggest effect on Real Time Kinematic (RTK) and Network RTK (NRTK) performance for Australian GNSS users, due mainly to their wavelength and amplitude. Despite the small amplitude of MSTIDs (typically tenths of a TECU), these ionospheric disturbances can cause a (sometimes dramatic) decrease in the performance of GNSS positioning (e.g. Wanninger, 2004; Wu et al., 2006). TIDs can also introduce biases in the ionospheric interpolation process applied within CORS networks with baselines from tens to hundreds of kilometres, due to the inability of routinely used models to account for these short-term fluctuations (Hernández-Pajares et al., 2006).

An increased number of ionospheric storms can be expected to occur during the upcoming solar maximum (Valladares et al., 2009). These storms are able to significantly degrade GNSS positioning accuracy, particularly during high solar activity (Skone, 2001). During an ionospheric storm in northern Europe, kinematic analysis of GNSS position repeatability has been shown to degrade by one order of magnitude, from better than 1 cm in the horizontal and about 2.5 cm in the vertical position to 12 cm in the horizontal and 26 cm in the vertical (Bergeot et al., 2011). This was attributed mainly to second-order ionospheric delays on GNSS signals which are currently not accounted for in routine GNSS data processing. It was also noted that this degradation was less severe for stations located in central Europe, again highlighting the strong latitude dependency of ionospheric effects.

5.2 Indications from Australian Studies

It is very difficult to quantify the effects of the approaching solar maximum on GNSS positioning users in Australia, mainly due to the complexity of the ionosphere and the lack of studies conducted in this region. In a rare example, Wu et al. (2006) investigated the temporal and spatial variations of the ionosphere over Victoria using GPS CORS data collected over a period of two years (2003 and 2004). It was found that maximum TEC values generally occur at about 14:00 local time, while minimum values are observed at about 03:00 local time. As expected, daytime TEC values were larger than night-time values. However, significant diurnal and seasonal ionospheric TEC variations were evident. In spring (September to November) and autumn (March to May), daytime TEC values were generally greater than in the other two seasons, i.e. summer (December to February) and winter (June to August). The study also revealed spatial correlations, in principle allowing ionosphere modelling across the entire state. However, the existence of TEC gradients causes difficulties in establishing an appropriate model that sufficiently describes the complex nature of ionospheric effects over such a wide area for high-precision, real-time GNSS positioning.

By using a regional CORS network, such as CORSnet-NSW (Janssen et al., 2011) or GPSnet (Hale et al., 2008), a large portion of the differential ionospheric biases can be modelled and removed. However, in the presence of small-scale or medium-scale ionospheric disturbances large ionospheric residuals can remain, even with NRTK. The advantage of NRTK over single-base RTK lies in the mitigation of the ionospheric biases affecting ambiguity resolution and positioning accuracy. The ionospheric correction models of NRTK successfully remove (at least) the linear part of the differential ionospheric biases (Wanninger, 2004). Connecting to a regional CORS network is therefore the preferred option in regards to minimising the effects of the approaching solar maximum on real-time GNSS surveys in Australia. However, it should be emphasised that ionospheric disturbances are also prone to affect the

communication links required to transfer data between the CORS network (or a local base station) and the GNSS user. As a result, radio links and mobile phone connections can suffer, at times leading to the need for more frequent reinitialisation of the GNSS receiver.

5.3 What Does the Future Hold?

Based on the findings of these recent studies, it is appropriate to speculate about how GNSS users and CORS network operators may be able to minimise the effects on GNSS positioning performance during solar maximum conditions in the near future.

GNSS users may be required to pay more attention to their rover and its real-time performance indicators over the next few years. It is well known that coordinate quality indicators are generally overly optimistic (e.g. Edwards et al., 2010; Janssen and Haasdyk, 2011). This discrepancy is likely to be more pronounced during heightened solar activity, leading to an increased number of outlier positions not identified by the rover's quality indicators.

The effect of ionospheric disturbances on GNSS positioning performance at the user end may differ between receiver brands and receiver types due to variations in receiver hardware, firmware and the algorithms employed (see section 5.1). This is likely to continue, as each manufacturer continues to develop improved ways of accounting for the ionospheric delay, e.g. via long-range RTK algorithms. As a result, the performance gap between legacy (GPS-only) equipment and modern GNSS rovers will grow considerably. In any case, it may be beneficial to increase observation times to obtain additional measurements if possible.

New algorithms for sparse CORS networks, allowing station separations of about 100 km or more, are now commercially available to CORS network providers. Applying these across existing, denser CORS networks may help to counter-balance at least some of the expected reduction in positioning quality due to the solar maximum, possibly resulting in current user performance to be maintained in some areas. In general, connecting to a CORS network using NRTK is recommended to help minimise the effects of ionospheric disturbances on real-time GNSS applications. The continuing expansion of regional CORS networks, paired with the introduction of new GNSS signals (see section 4), will significantly improve ionospheric modelling in the near future. This, in turn, will minimise the effects of the solar maximum on modern GNSS equipment.

6 CONCLUDING REMARKS

This paper has briefly reviewed how the solar cycle influences the behaviour of the ionosphere and described related phenomena such as scintillations, travelling ionospheric disturbances and ionospheric storms. Recent advances in modelling the ionosphere have been outlined, and the likely effects of the approaching solar maximum of cycle 24 (currently predicted to occur in early 2013) on GNSS users have been discussed.

GNSS users should be alert but not alarmed. GNSS positioning is expected to continue to perform at current levels most of the time, with the occasional larger and more frequent glitches encountered in the field. Australia is located mainly in the mid-latitude region and therefore generally spared from the most severe ionospheric disturbances. In addition, the approaching solar maximum is predicted to be significantly smaller than the previous peak in

2000-2001. However, it should be noted that many of the most intense solar outbursts have occurred during below-average solar cycles. During the solar maximum period, which may last for up to two years or so (i.e. until about 2015), intermittent degradation of positioning performance (particularly for real-time surveys) should be anticipated across Australia. An increased number of cycle slips and periods of frequent loss-of-lock to multiple satellites are expected to occur at times. In addition, drop-outs in the communication links required for real-time applications (i.e. radio link or connection to mobile internet) should be anticipated. GNSS users in Northern Australia can expect more severe scintillation effects to occur more frequently. Consequently, GNSS users should pay particular attention to GNSS best practice and be a little more cautious over the next few years.

The gap of about 11 years between solar maxima marks only one iteration of the solar cycle, but it represents several generations in regards to GNSS infrastructure and receiver design. The number and density of GNSS CORS networks in operation has increased considerably since the previous solar maximum, both at global and regional scales. In addition, significant progress has been made in ionospheric modelling. As a result, the GNSS community is well prepared for the approaching solar maximum. This also provides an unprecedented opportunity to further enhance our understanding of the complex nature of the ionosphere and to develop and test improved ionospheric models (e.g. higher resolution and lower latency) using the CORS data collected over the next few years.

Efficient real-time modelling of the ionospheric effects on GNSS observations is getting close to becoming a reality. The growing number of operational GNSS constellations will not only contribute to this process, but also help generate new alternatives for GNSS positioning which may be less affected by variations in the ionosphere.

REFERENCES

AIUB (2012) Global ionosphere maps produced by CODE, http://www.aiub.unibe.ch/content/research/gnss/code__research/igs/global_ionosphere_maps_produced_by_code/ (accessed Jan 2012).

Allain D.J. and Mitchell C.N. (2009) Ionospheric delay corrections for single-frequency GPS receivers over Europe using tomographic mapping, *GPS Solutions*, 13(2), 141-151.

Anderson D. and Fuller-Rowell T. (1999) Space environment topics: The ionosphere, SE-14, Space Environment Center, Boulder, Colorado, http://www.sec.noaa.gov/Education/ (accessed Feb 2012).

Bergeot N., Bruyninx C., Defraigne P., Pireaux S., Legrand J., Pottiaux E. and Baire Q. (2011) Impact of the Halloween 2003 ionospheric storm on kinematic GPS positioning in Europe, *GPS Solutions*, 15(2), 171-180.

Bilitza D. (2006) The International Reference Ionosphere – Climatological standard for the ionosphere, *Proceedings of RTO-MP-IST-056*, Neuilly-sur-Seine, France, 12-16 June, paper 32, 12pp.

Burrell A.G., Bonito N.A. and Carrano C.S. (2009) Total electron content processing from GPS observations to facilitate ionospheric modeling, *GPS Solutions*, 13(2), 83-95.

Bust G.S. and Mitchell C.N. (2008) History, current state, and future directions of ionospheric imaging, *Reviews of Geophysics*, 46, RG1003, doi:10.1029/2006RG000212.

Chen W., Gao S., Hu C., Chen Y. and Ding X. (2008) Effects of ionospheric disturbances on GPS observation in low latitude area, *GPS Solutions*, 12(1), 33-41.

Chen W., Hu C., Chen Y., Ding X. and Kowk S.C. (2001) Rapid static and kinematic positioning with Hong Kong GPS active network, *Proceedings of ION GPS 2001*, Salt Lake City, Utah, 11-14 September, 346–352.

Datta-Barua S., Doherty P.H., Delay S.H., Dehel T. and Klobuchar J.A. (2003) Ionospheric scintillation effects on single and dual frequency GPS positioning, *Proceedings of ION GPS/GNSS 2003*, Portland, Oregon, 9-12 September, 336-346.

Doherty P.H., Delay S.H., Valladares C.E. and Klobuchar J.A. (2000) Ionospheric scintillation effects in the equatorial and auroral regions, *Proceedings of ION GPS 2000*, Salt Lake City, Utah, 19-22 September, 662-671.

Edwards S.J., Clarke P.J., Penna N.T. and Goebell S. (2010) An examination of Network RTK GPS services in Great Britain, *Survey Review*, 42(316), 107-121.

ESA (2005) The ionosphere explained, EGNOS fact sheet no. 2, http://www.egnos-pro.esa.int/Publications/2005%20Updated%20Fact%20Sheets/fact_sheet_2.pdf (accessed Feb 2012).

Gao Y. and Liu Z.Z. (2002) Precise ionosphere modeling using regional GPS network data, *Journal of Global Positioning Systems*, 1(1), 18-24.

Goodman J.M. and Aarons J. (1990) Ionospheric effects on modern electronic systems, *Proceedings of the IEEE*, 78(3), 512-528.

Hale M., Collier P. and Kealy A. (2008) GPSnet CORS network management validation through user feedback, *Journal of Spatial Science*, 53(2), 97-113.

Hernández-Pajares M., Juan J.M. and Sanz J. (2006) Medium-scale traveling ionospheric disturbances affecting GPS measurements: Spatial and temporal analysis, *Journal of Geophysical Research*, 111, A07S11, doi:10.1029/2005JA011474.

Hernández-Pajares M., Juan J.M., Sanz J. and Orús R. (2007) Second-order ionospheric term in GPS: Implementation and impact on geodetic estimates, *Journal of Geophysical Research*, 112, B08417, doi:10.1029/2006JB004707.

Hocke K. and Schlegel K. (1996) A review of atmospheric gravity waves and traveling ionospheric disturbances: 1982-1995, *Annales Geophysicae*, 14(9), 917–940.

Hoque M.M. and Jakowski N. (2008) Estimate of higher order ionospheric errors in GNSS positioning, *Radio Science*, 43, RS5008, doi:10.1029/2007RS003817.

IPS (2012a) Solar cycle, http://www.ips.gov.au/Educational/2/3 (accessed Feb 2012).

IPS (2012b) Introduction to HF radio propagation, http://www.ips.gov.au/Educational/5/1 (accessed Feb 2012).

IPS (2012c) TEC regional map, http://www.ips.gov.au/Satellite/2/1 (accessed Jan 2012).

Janssen V. and Haasdyk J. (2011) Assessment of Network RTK performance using CORSnet-NSW, *Proceedings of IGNSS2011*, Sydney, Australia, 15-17 November, 18pp.

Janssen V., Haasdyk J., McElroy S. and Kinlyside D. (2011) CORSnet-NSW: Improving positioning infrastructure for New South Wales, *Proceedings of SSSC2011*, Wellington, New Zealand, 21-25 November, 395-409.

Janssen V. and Rizos C. (2003) Processing mixed-mode GPS networks for deformation monitoring applications, *zfv* (Journal of Geodesy, Geoinformation and Land Management), 128(2), 87-96.

Jensen A.B.O. and Mitchell C. (2011) GNSS and the ionosphere: What's in store for the next solar maximum? *GPS World*, 22(2), 40-48.

Kintner P.M., Humphreys T. and Hinks J. (2009) GNSS and ionospheric scintillation: How to survive the next solar maximum, *Inside GNSS*, 4(4), 22-31.

Klobuchar J.A. (1987) Ionospheric time-delay algorithm for single-frequency GPS users, *IEEE Transactions on Aerospace and Electronic Systems*, 23(3), 325-331.

Klobuchar J.A. (1996) Ionospheric effects on GPS, in: Parkinson B.W. and Spilker J.J. (Eds.) *Global Positioning System: Theory and Applications Volume I*, Progress in Astronautics and Aeronautics, 163, American Institute of Aeronautics and Astronautics, Washington, 485-515.

Knight M. (2000) Ionospheric scintillation effects on Global Positioning System receivers, PhD Dissertation, Department of Electrical and Electronic Engineering, The University of Adelaide, Australia, 304pp.

Kotake N., Otsuka Y., Ogawa T., Tsugawa T. and Saito A. (2007) Statistical study of medium-scale traveling ionospheric disturbances observed with the GPS networks in Southern California, *Earth Planets Space*, 59(2), 95-102.

Kunches J.M. and Klobuchar J.A. (2001) Eye on the ionosphere: GPS after SA, *GPS Solutions*, 4(3), 52-54.

Langley R.B. (2000) GPS, the ionosphere, and the solar maximum, *GPS World*, 11(7), 44-49.

Liu J., Chen R., Wang Z. and Zhang H. (2011) Spherical cap harmonic model for mapping and predicting regional TEC, *GPS Solutions*, 15(2), 109-119.

NASA (2012a) The very latest SOHO images, http://sohowww.nascom.nasa.gov/data/realtime-images.html (accessed Jan 2012).

NASA (2012b) Solar cycle prediction, http://solarscience.msfc.nasa.gov/predict.shtml (accessed Mar 2012).

Richert T. and El-Sheimy N. (2005) Ionospheric modeling: The key to GNSS ambiguity resolution, *GPS World*, 16(6), 6pp.

Rizos C. (2008) Multi-constellation GNSS/RNSS from the perspective of high accuracy users in Australia, *Journal of Spatial Science*, 53(2), 29-63.

Roberts C. (2011) How will all the new GNSS signals help RTK surveyors? *Proceedings of SSSC2011*, Wellington, New Zealand, 21-25 November, 411-423.

Schaer S., Beutler G. and Rothacher M. (1998) Mapping and predicting the ionosphere, *Proceedings of IGS AC Workshop*, Darmstadt, Germany, 9-11 February, 12pp.

Schüler T., Diessongo H. and Poku-Gyamfi Y. (2011) Precise ionosphere-free single-frequency GNSS positioning, *GPS Solutions*, 15(2), 139-147.

Seeber G. (2003) *Satellite Geodesy* (2nd edition), de Gruyter, Berlin, Germany, 589pp.

Seo J., Walter T., Marks E., Chiou T.-Y. and Enge P. (2007) Ionospheric scintillation effects on GPS receivers during solar minimum and maximum, *Proceedings of International Beacon Satellite Symposium 2007*, Boston, Massachusetts, 11-15 June, 6pp.

Skone S.H. (2001) The impact of magnetic storms on GPS receiver performance, *Journal of Geodesy*, 75(6), 457-468.

Solanki S.K. (2003) Sunspots: An overview, *The Astronomy and Astrophysics Review*, 11(2-3), 153-286.

Teunissen P.J.G. and Kleusberg A. (Eds.) (1998) *GPS for Geodesy* (2nd edition), Springer, Berlin, 650pp.

Tsugawa T., Otsuka Y., Coster A.J. and Saito A. (2007) Medium-scale traveling ionospheric disturbances detected with dense and wide TEC maps over North America, *Geophysical Research Letters*, 34, L22101, doi:10.1029/2007GL031663.

Valladares C.E., Villalobos J., Hei M.A., Sheehan R., Basu S., MacKenzie E., Doherty P.H. and Rios V.H. (2009) Simultaneous observation of traveling ionospheric disturbances in the northern and southern hemispheres, *Annales Geophysicae*, 27(4),1501-1508.

Wang M., Ding F., Wan W., Ning B. and Zhao B. (2007) Monitoring global traveling ionospheric disturbances using the worldwide GPS network during the October 2003 storms, *Earth Planets Space*, 59(5), 407-419.

Wanninger L. (2004) Ionospheric disturbance indices for RTK and Network RTK positioning, *Proceedings of ION GNSS 2004*, Long Beach, California, 21-24 September, 1849-2854.

Wielgosz P., Grejner-Brzezinska D., Kashani I. and Yi Y. (2003) Instantaneous regional ionosphere mapping, *Proceedings of ION GPS/GNSS 2003*, Portland, Oregon, 9-12 September, 1750-1757.

Wu S., Zhang K., Yuan Y. and Wu F. (2006) Spatio-temporal characteristics of the ionospheric TEC variation for GPSnet-based real-time positioning in Victoria, *Journal of Global Positioning Systems*, 5(1), 52-57.

Ya'acob N., Abdullah M. and Ismail M. (2008) Determination of GPS total electron content using single layer model (SLM) ionospheric mapping function, *International Journal of Computer Science and Network Security*, 8(9), 154-160.